Synthesis and Antibiotic Activity of Chitosan-Based Comb-Like Co-Polypeptides

Timothy P. Enright , Dominic L. Garcia , Gia Storti , Jason E. Heindl , Alexander Sidorenko *

Posted Date: 10 March 2023

doi: 10.20944/preprints202303.0189.v1

Keywords: Antimicrobial peptides; Chitosan; comb-like co-polypeptide; N-carboxyanhydrides; ring-opening polymerization

Article

Synthesis and Antibiotic Activity of Chitosan-Based Comb-Like Co-Polypeptides

Timothy Enright [1], Dominic Garcia [1], Gia Storti [1], Jason Heindl [2] and Alexander Sidorenko [1,*]

[1] Saint Joseph's University, Department of Chemistry and Biochemistry, Philadelphia, PA.
[2] Department of Biological & Biomedical Sciences, Rowan University, Glassboro, NJ.
* Correspondence: asidorenko@sju.edu

Abstract: The development of antimicrobial resistance to conventional antibiotics is a major global health challenge. Infections caused by multidrug-resistant gram-negative bacteria have been named one of the most urgent global health threats. Considerable efforts are devoted to developing new antibiotic drugs and investigating the mechanism of antibiotic resistance. Recently, Anti-Microbial Peptides (AMPs) have emerged as a new platform for the target and design of novel drug resistant anti-microbial agents promising a new therapeutic strategy. AMPs are rapid, potent, possess an unusually broad spectrum of activity, and have shown efficacy as topical agents. Unlike traditional therapeutics that interfere with essential bacterial enzymes, AMPs interact with microbial membranes through electrostatic interactions and physically damage cell integrity. However, naturally occurring AMPs have limited selectivity and modest efficacy. Therefore, recent efforts have focused on the development of synthetic AMP analogs as suitable drug targets. This work explores the development of novel antimicrobial agents which mimic the structure of graft-copolymers and mirror the mode of action of an AMP. Chitosan-graft-polypeptide side chains are synthesized by the ring-opening polymerization of N-carboxyanhydrides of L-lysine and L-leucine initiated from the functional groups of chitosan. The derivatives with random- and block-copolymer side chains are explored as drug targets. These graft copolymer systems exhibit activity against clinically significant pathogens and disrupt biofilm formation. This work highlights the potential of chitosan-graft-polypeptide structures in biomedical applications.

Keywords: antimicrobial peptides; chitosan; comb-like co-polypeptide; N-carboxyanhydrides; ring-opening polymerization

1. Introduction

Antimicrobial peptides (AMPs) are a unique class of peptides that are part of the innate immune response of most multicellular organisms [1]. Unlike traditional antibiotics, which inhibit an intracellular target, AMPs and their synthetic analogues rely on physically damaging the bacterial cell membrane [2]. As such, they offer promise as a versatile therapeutic to combat the rising trend of antimicrobial resistance. The AMPs with a broad range of structural and chemical compositions have been identified [3]. However, several characteristics are conserved [4]: effective AMPs possess a net positive charge, hydrophobic moieties, and amphiphilicity. Some approaches for improving the pharmacological performance of naturally derived AMPs have included chemical modification [5], non-native amino acids [6], fully or semi-synthetic scaffolds [7-10], supramolecular assembly [11, 12], and multimeric structures [13, 14]. The rational design of synthetic analogues may facilitate further improvement of the pharmacodynamic properties. In particular, grafting peptides to a common polymer backbone to create an antimicrobial graft copolymer (GCP) may bring several advantages: (i) they provide an opportunity to incorporate various functionalities and tune parameters to achieve high activity, e. g. hydrophilic/hydrophobic balance; (ii) the graft copolymer structure provides a high local concentration of peptides which may facilitate bacteria membrane disruption thus reducing minimally required global concentration as compared to traditional AMPs; (iii) the redundancy of GCP's peptide grafts may undergo conformational adjustment to maximize favorable interactions with the local environment and facilitate penetration of the GCP in the bacteria cell wall and promote cell death; (iv) the composition of the GCPs can be selected to complement the

Preprints (www.preprints.org) | NOT PEER-REVIEWED | Posted: 10 March 2023 doi:10.20944/preprints202303.0189.v1

peptidoglycan layer of the cytoplasmic membrane of a bacteria. A complementary structure may improve selectivity over mammalian cells and promote adsorption onto the cell wall of bacteria [15]. Despite the large number of studies demonstrating the therapeutic potential of AMP-based therapeutics, only a few candidates have made it through the discovery phase and found clinical application [16].

In this work we report the synthesis of novel antimicrobial GCPs and evaluate their antibacterial activity. We use a natural polysaccharide chitosan (CHI) as a backbone to fabricate a small library of peptide graft-copolymers via ring-opening polymerization (ROP) of N-carboxyanhydrides (NCA) of L-lysine and L-leucine. Graft copolymers with branched architectures composed of homo-, random, and block-polypeptide sequences have been targeted. The graft copolymers are characterized by NMR, IR, SEC, and MS, and their molecular weight, composition, and architecture are evaluated. The results of i*n vitro* investigation of antibacterial activity against model pathogens and cytotoxicity for human dermal fibroblasts are reported. Finally, we assess the effect of the GCPs on the biomass and cell viability within biofilms of *Agrobacterium tumefaciens* (*A. tumefaciens*).

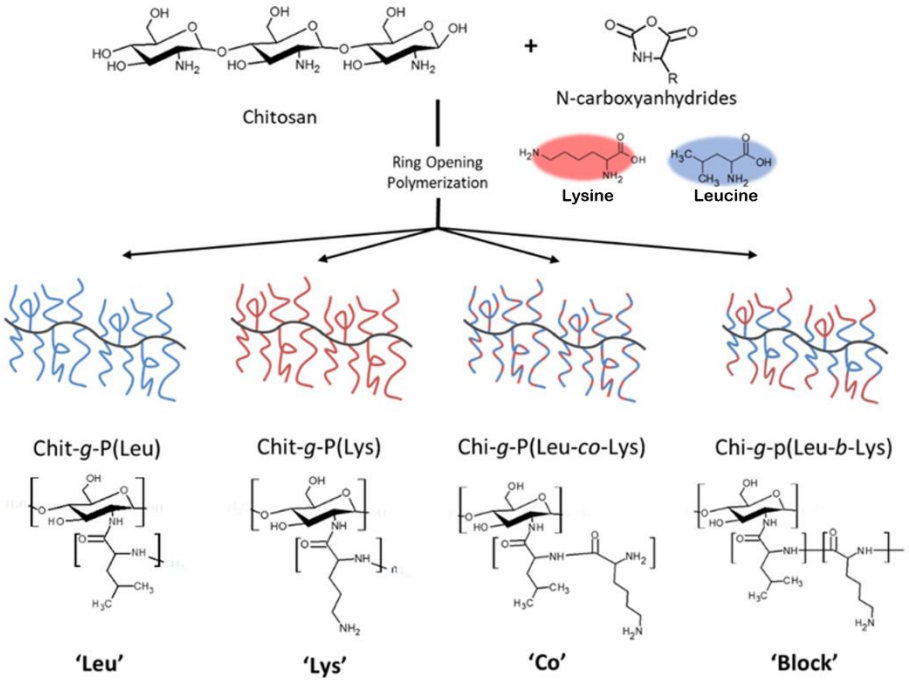

Figure 1. Synthetic methodology developed to fabricate a cationic peptidopolysaccharide graft copolymers consisting of L-lysine and L-leucine oligomers conjugated to chitosan via ring-opening polymerization of N-carboxyanhydrides (NCA-ROP).

2. Materials and Methods

i. Materials

Chitosan of low molecular weight (Brookfield viscosity 20-300 cP, for 1 wt.% in 1% acetic acid; Mv= 50-190 kDa; 90% deacetylated), 10-camphorsulfonic acid (β) (CSA, 98%), N,N-diisopropylethylamine (DIPEA, 99.5%), D-(+)-glucosamine hydrochloride (GlcN, >99%), N-acetyl-D-glucosamine, (GlcNAc, >98%), 3-nitrobenzonitrile (3-NBN, 98%), were purchased from Millipore Sigma and used as is. N_6-carbobenzyloxy-l-lysine (H-Lys(Z)-OH, 98%) and triphosgene (>99%) were purchased from Oakwood chemical Inc. (4S)-4-(2-methylpropyl)-1, 3-oxazolidine-2, 5-dione (L-leucine-NCA) of 98% purity was purchased from OXCHEM corporation. Dimethyl sulfoxide (DMSO) and tetrahydrofuran (THF) were dried over 3Å molecular sieves to remove water and stored under argon until use. All other solvents were of analytical grade and used without further purification. Glassware used for NCA synthesis and polymerization were dried at 120ºC under vacuum overnight.

 doi:10.20944/preprints202303.0189.v1

Magainin and Müeller-Hinton media/agar were purchased from Sigma Aldrich. alamarBlue™ Cell Viability Reagent and MTT (3-(4,5-Dimethylthiazol-2-yl)-2,5-Diphenyltetrazolium Bromide) was purchased from ThermoFisher Scientific. All other materials and supplies were purchased from MilliporeSigma.

The following established bacterial strains were used in this study, all of which are included in our strain collection: *Agrobacterium tumefaciens* strain C58 and its isogenic deletion derivatives lacking either *visR* or the *upp* loci [17, 18], *Escherichia coli* strain BW21553 (Coli Genetic Stock Center), and *Staphylococcus aureus* strain F-182 (American Type Culture Collection).

ii. Methods

Synthesis of CHI-CSA salt

Using a method adapted from Sashiwa *et al.*[19], 10-camphorsulfonic acid salt of chitosan (CHI-CSA) was prepared as follows. Chitosan (5g, 30 mmol of NH_2) was suspended in 1L of water and 10-camphorsulfonic acid (CSA) (7.3 g) in an equimolar amount to NH_2 of CHI was added. The suspension was stirred until a clear solution formed (approx. 1 h). The solution was coarsely filtered and dialyzed in a cellulose membrane (MW cut-off 12,000 Da) against Milli-pure water for 3 days. The solution was then lyophilized to a fluffy white solid and stored under argon.

Synthesis of L-lysine(Z)-NCA

H-Lys(Z)-OH (1.5 g, 5.3 mmol) was dried under vacuum and added to 50 ml of anhydrous ethyl acetate in a dried round bottom flask under argon. Triphosgene (0.8 g, 2.7 mmol) was added to the suspension and the mixture was heated to 60°C at continuous stirring for 3 h. Upon the formation of a clear solution, the reaction was cooled to 0°C and extracted with water until a neutral pH of the aqueous phase was achieved. The purified organic phase was dried with $MgSO_4$ and the solvent was removed under vacuum. The resulting white solid was recrystallized from THF: hexane (1:3) to remove any residual triphosgene and dried under high vacuum overnight to obtain L-lysine(Z)-NCA. Yield: 1.6 g, (75%).

Synthesis of L- Lysine (TFA) NCA

N_ε-Trifluoroacetyl-L-lysine (2.4g, 10 mmol) was suspended in 100 ml anhydrous ethyl acetate under argon. Triphosgene (1.0 g, 3.3 mmol) was added to the suspension and heated to 40°C while stirring overnight. Upon the formation of a clear solution, the crude NCA was precipitated using anhydrous pentane (100 ml) and washed 3 times with additional pentane. The resulting white solid was dried under high vacuum at ambient temperature. Yield: 2.3 g, (85%)

Synthesis of L-leucine-NCA

Using a method adapted from Smeets *et al.* [20], L-Leucine (2.5 g, 17 mmol) was suspended in anhydrous THF (100 ml) in a dry 250 ml round bottom flask. The suspension was heated to 50°C while stirring and triphosgene (1.8 g, 6 mmol) was added under a steady flow of argon. The reaction proceeded for 120 min at which time a clear solution was obtained. The solution was cooled and the solvent was evaporated under reduced pressure, yielding an off-white solid. The crude L-leucine NCA was dissolved in toluene and recrystallized using a minimal amount of n-heptane. The final product appeared as transparent needle-like crystals. Yield 2.0 g, (76%)

Synthesis of CHI-graft-Poly(L-lysine(Z))

In a dry 250 ml round bottom flask CHI-CSA (0.8 g, 2.0 mmol) was dissolved in 125 ml of anhydrous DMSO and equipped with a stir bar. Once dissolved, a three-fold excess L-lysine(Z)-NCA (1.87 g, 6.1 mmol) was added to the solution. The reaction proceeded at 23°C while stirring over a period of 5 days. CHI-*graft*-Poly(lysine(Z)) polymer solution was isolated by precipitation in diethyl

 doi:10.20944/preprints202303.0189.v1

ether (3 x 100ml) and collected by centrifugation. The resulting residue was dried under vacuum to yield a white solid, 1.78 g (74%).

Synthesis of CHI-graft-Poly(lysine(Z)-co-leucine)

Synthesis was carried out in a similar fashion to CHI-*graft*-Poly(lysine(Z)). In a dry 250 ml round bottom flask CHI-CSA (0.8g, 2.0 mmol) was dissolved in 125 ml of anhydrous DMSO and equipped with a stir bar. Once dissolved, L-lysine(Z)-NCA (0.937g, 3.0 mmol) and L-leucine-NCA (0.479 g, 3.0 mmol) were added to the solution in a 1.5-fold molar excess to CHI's amines. The reaction proceeded over 5 days and the final product was isolated by precipitation in diethyl ether and collected by centrifugation. The resulting residue was dried under vacuum to yield a white solid, 0.74 g (49%).

Synthesis of CHI-graft-Poly(leucine-block-lysine(Z))

Using the method described above, CHI-*graft*-Poly(leucine) was first synthesized. In a dry round bottom flask 0.69g of CHI-*graft*-Poly(leucine) was dissolved in 125 ml of anhydrous DMSO and equipped with a stir bar. Once dissolved, L-lysine(Z)-NCA (1.64 g, 5.3 mmol) was added to the solution. The reaction proceeded at 23°C while stirring over a period of 5 days. The CHI-block-polypeptide product was isolated by precipitation in diethyl ether and collected by centrifugation. The resulting residue was dried under vacuum to yield a white solid, 0.76 g (55%).

Synthesis of linear GlcN-term-Poly(lysine(Z))

In a dry 250 ml round bottom flask 1.5 mmol of GlcN or GlcNAc was dissolved in 125 ml of anhydrous DMSO and equipped with a stir bar. Once dissolved, a 3-fold excess of NCAs (4.5 mmol) was added to the solution. The reaction proceeded at 23°C while stirring over a period of 5 days. The final products were isolated by precipitation in diethyl ether and collected by centrifugations residue was dried under high vacuum overnight to yield off-white solids.

Deprotection of N-ε-Carbobenzyloxy-L-lysine (L-lysine(Z)) moieties

N-ε-Carbobenzyloxy-L-lysine products were deprotected by HBr. Generally, 1.0 g of polymer was dissolved in 15 mL of Trifluoroacetic acid at 0°C in a sealed vessel. Once dissolved, 15mL of HBr (33% in acetic acid) was added and stirred for 45 minutes. The polymer was precipitated with diethyl ether (150 ml) the collected by centrifugation. The final product was washed two additional times with diethyl ether and dried under high vacuum to yield and off-white solid.

iii. Characterization

Size exclusion chromatography (SEC) was used to characterize the molecular weight of the GCPs and model linear polypeptides GlcN-*term*-Poly(lysine). SEC analysis was performed using a Perkin-Elmer Series 200 HPLC/SEC with a 785A UV/Vis detector set at 210 nm. The column used was GRAM from PSS Polymer Standards Service GmbH, Germany. DMF was used as a mobile phase for analysis. 1% solutions of the GCPs and model linear polypeptides were filtered through a 0.2 μ filter and used for SEC. The flow rate for analysis was 0.5 mL/min at 40°C, and the sample size was 40 μL.

1H-NMR spectroscopy was performed at room temperature using a Bruker Advance III (400 MHz) NMR spectrometer and analyzed with TopSpin software. Spectra of the products were evaluated against precursors typically with DMSO-d6 as a reference.

IR spectra was collected using a Nicolet iS10 FTIR spectrophotometer with a Smart iTX Diamond ATR accessory from 4000cm-1 to 400cm-1. Each experiment used 32 scans.

Minimum inhibitory concentrations (MICs)

Bacteria cells were grown overnight at 37°C in Müeller-Hinton (MH) media to a mid-log phase and diluted to 10^4 to 10^5 CFU ml^{-1} in media. A twofold dilution series of 100 μL drug solution in the MH media was made on 96-well microplate, followed by the addition of 5 μL bacterial suspension

Preprints (www.preprints.org) | NOT PEER-REVIEWED | Posted: 10 March 2023 doi:10.20944/preprints202303.0189.v1

(10^4 to 10^5 CFU mL^{-1}). The plates were incubated at 37°C for 18 h, and the absorbance at 600 nm was measured with a microplate reader (BioTek Synergy HT). Additionally, 10 µl of AlamarBlue Cell viability reagent assay was added to each well and incubated at 37°C for an additional 2 h. The absorbance at 570 nm was measured. Positive control measurements were performed without product, and negative control was done without bacteria/ inoculum. MICs were determined as the lowest concentration that inhibited cell growth by 90% using curve-fitting.

LIVE/DEAD Assay to examine bacterial viability

The number of viable cells after exposure to test compounds was confirmed by serially diluting aliquots of bacteria in Müeller-Hinton media and plating onto Müller-Hinton Agar for *A. tumefaciens*. The plates were incubated overnight and numbers of live bacteria were enumerated and expressed as CFU ml^{-1}. Experiments were performed in triplicate.

Crystal violet biofilm assay

Static-culture biofilms were grown on sterile PVC coverslips suspended vertically in the wells of UV-sterilized 12-well polystyrene dishes. Overnight cultures were diluted to an initial optical density at 600 nm (OD_{600}) of 0.05 in ATGN media. Each well was inoculated with 3 ml of culture, and the dishes were incubated at room temperature for 12 to 96 h. Coverslips were stained with 0.1% crystal violet (CV) dye. Quantification of adherent biomass was achieved via solubilization of adsorbed CV with 33% acetic acid. The OD_{600} of the 48-h planktonic cultures and the A_{600} of the solubilized adherent CV were measured with a plate reader BioTek Synergy HT. Values shown are the mean A_{600} +/- standard error of three biofilm cultures for each strain/condition.

3. Results and Discussion

Synthesis of Chitosan-based GCPs

The chitosan backbone was prepared using a method adopted by Sashiwa et al [19]. For complete dissolution to take place the CHI-CSA salt was freeze-dried. The solid was found to readily dissolve in DMSO. With this development further chemical modification of CHI could be carried out in homogeneous water-free conditions. Many factors in sourcing and manufacturing CHI affect the characteristics and composition of the final product. Since the amino groups of CHI initiate grafting, it is important to establish the fraction of available amino groups prior to modification. ^{1}H NMR spectrum of CHI-CSA in DMSO-d_6 is presented in Figure 2. The signals at 3.5 ppm, 4.8 ppm, and 8.3 ppm are attributed to the -5, -1, and -NH_2 hydrogens of CHI, respectively. The hydrogens bound to the pyranose ring (3, 4, 5, and 6) are assigned to a broad peak at about 3.8 ppm.

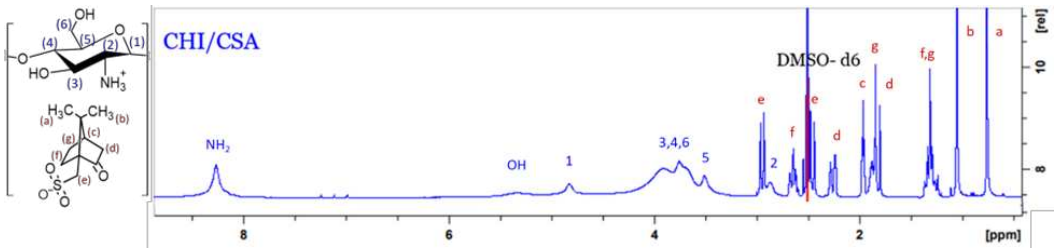

Figure 2. ^{1}H-NMR spectrum of the CHI-CSA in DMSO-d6 with schematic presentation of repeat unit.

The degree of acetylation was calculated using a method proposed by Weinhold et al., where the area of the acetyl CH_3 hydrogens (A_{CH_3}), and the H2-H6 signals (A_{H2-H6}) of CHI are used according to Eq. 1 [21]:

Preprints (www.preprints.org) | NOT PEER-REVIEWED | Posted: 10 March 2023 doi:10.20944/preprints202303.0189.v1

$$\%DA = \left[1 - \left(\frac{\frac{1}{3} * A_{CH_3}}{\frac{1}{6(A_{H2-H6})}}\right)\right] * 100 \quad (1)$$

The %DA was found to be > than 99%. Literature reports that N-acetyl linkages, as well as main chain (glycosidic linkages) of CHI, are susceptible to acidic hydrolysis [22]. It is likely that during the dissolution of CHI the acetyl groups are cleaved while in the presence of excess CSA.

CHI-graft-polypeptides could yield a versatile material with the combined characteristics of its components, tunable amphiphilicity, and potentially controlled interactions with the environment. Several research groups have synthesized such materials using the amino group of CHI to initiate ROP of amino acid NCAs (Figure 3). However, the restricted solubility of CHI limits the number of synthetic pathways. Kurita et al. and Chi et al. synthesized CHI-g-poly(γ-methyl L-glutamate) and CHI-g-poly(L-lysine) using a biphasic interfacial approach in ethyl acetate and water [23, 24]. Alternatively, the synthesis of CHI-g-Poly(l-glutamic) acid and Poly(lysine-ran-phenylalanine) copolymers was accomplished in homogenous conditions using a soluble form of CHI, 6-O-triphenylmethyl CHI, in anhydrous DMF [25]. In this work, we adopted an approach first utilized by Perdith et al. [26] who synthesized CHI-graft-poly(sodium-L-glutamate) nanoparticles using the primary amine sulfonate salt, CHI-CSA, as a macroinitiator in DMSO. Extending this strategy, we explored the synthesis of CHI based GCPs with a hydrophobic L-leucine and cationic hydrophilic L-lysine amino acids.

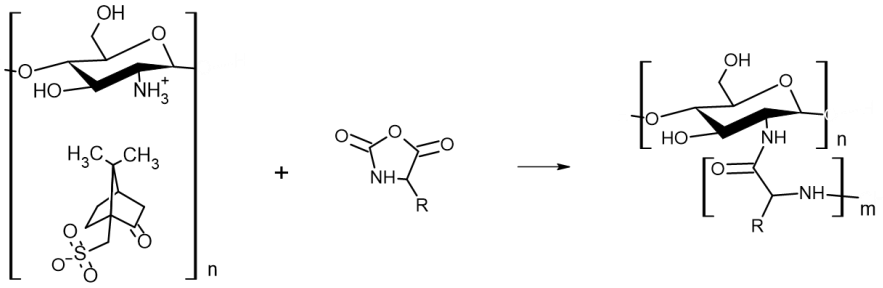

Figure 3. NCA-ROP synthesis of CHI based GCPs.

The CHI-CSA was rapidly dissolved under argon in dry DMSO to which 0.3 molar equivalents of DIPEA with respect to $-NH_3^+$ of CHI-CSA was added. The addition of DIPEA served to suppress acid-catalyzed cleavage of chitosan and increase the propagation rate of NCA-ROP. Control over the reactivity of the growing polymer chain end is critical to achieve a high molecular weight with optimal conditions often necessary to be determined empirically. Amine salts such as CHI-CSA have diminished reactivity as a nucleophile due to the formation of the inactive protonated amines $-NH_3^+$. Polymerizations initiated with hydrochloride salts were found to yield single NCA addition and required elevated temperatures to proceed [27, 28]. Since CHI degrades in the presence of sulfonic acids, we adjusted the equilibrium of free amines by adding the base instead of temperature (Figure 4). DIPEA was selected as it is a sterically hindered base capable of scavenging protons without acting as a nucleophile. The addition of 0.3 equivalents of DIPEA to individual ammonium group of CHI-CSA was found to effectively yield graft copolymers after 3 days at room temperature. Upon completion the products were precipitated with diethyl ether and sequentially washed with THF and water to remove any starting materials and bi-products.

Preprints (www.preprints.org) | NOT PEER-REVIEWED | Posted: 10 March 2023 doi:10.20944/preprints202303.0189.v1

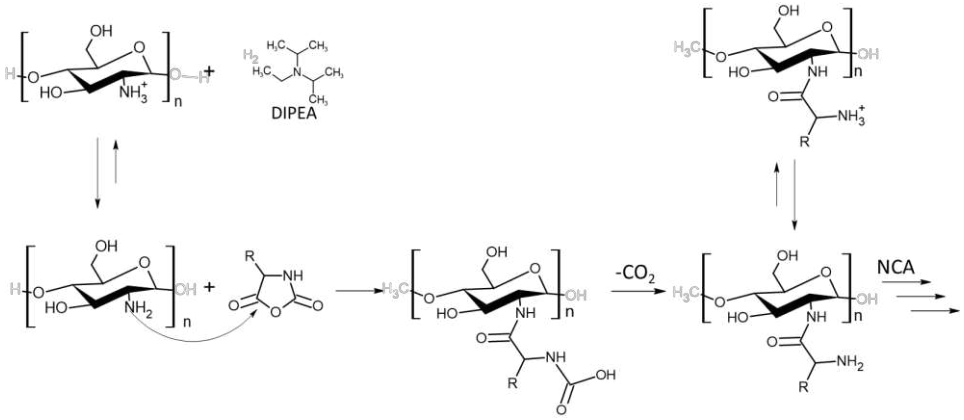

Figure 4. Tentative mechanism of the NCA-ROP using CHI-CSA as macroinitiator.

Synthesis of CHI-graft-Poly(L-lysine(Z))

Synthesis of CHI-graft-Poly(L-lysine(Z)) was carried out in standard conditions using a Cbz-protected form of L-lysine, N-ε-Carbobenzyloxy-L-lysine NCA (L-lysine(Z)-NCA). The ratio between the CHI and L-lysine(Z) NCA repeating units (CHI:Lys) was estimated by dividing the normalized integral value of the CHI protons 3H–6H (5 protons) by normalized integral value of the L-lysine(Z) B signal (6 protons) (Figure 5). A ratio of 1:0.43 for CHI to aliphatic lysine protons was found according to the Eq. 2:

$$Chi{:}\,Lysine = \left[\left(\frac{\frac{1}{5}*A_{Pyranose}}{\frac{1}{6\left(B_{Lys\ Akly}\right)}}\right)\right] \quad (2)$$

where, $A_{pyranose}$ is the area of 5 protons of the pyranose ring of CHI, B_{Akyl} is the area of 6 aliphatic protons of L-lysine, and $A_{Lys\ A}$ is the area of the 2 remaining aliphatic protons of L-lysine.

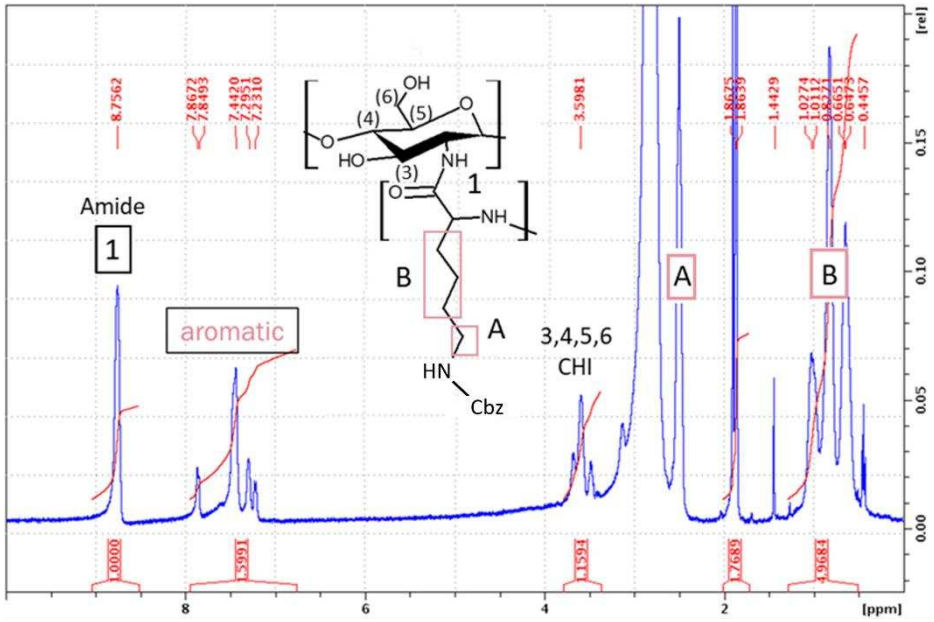

Figure 5. ^{1}H NMR spectra (d6-DMSO) of CHI-graft-Poly(L-lysine(Z)).

The Cbz protecting groups of L-lysine(Z) units were removed in two sequential deprotection reactions using HBr/AcOH and TFA. This yielded a water-soluble product rich in NH_2 functionalities, the deprotection degree was found to be 62% using Eq. 3:

Preprints (www.preprints.org) | NOT PEER-REVIEWED | Posted: 10 March 2023 doi:10.20944/preprints202303.0189.v1

$$\%Deprotection = \left[1 - \left(\frac{\frac{1}{5} * A_{aromatic}}{\frac{1}{2(A_{Lys\ A})}}\right)\right] * 100 \quad (2)$$

where $A_{aromatic}$ is the area of the 5 aromatic protons of the benzyloxycarbonyl protecting group of L-lysine(Z).

Synthesis of CHI-graft-poly(lysine-co-leucine)

Following the established procedure, CHI-graft-poly(L-lysine-co-L-leucine) was synthesized by copolymerization of NCA L-lysine and L-leucine in the presence of CHI for a 49% yield. A feed ratio of 1:1.5:1.5 (CHI-to-Lys-to-Lue) was selected so that the total NCA concentration remained consistent. As stated previously, L-leucine was selected as the hydrophobic component of the GCP. Additionally, L-Leucine allows for straightforward characterization of L-lysine(Z) deprotection as its proton resonances do not overlap with the aromatic protons of the Cbz protecting group. Upon work up the ratio of amino acids to CHI was determined with ^{1}H NMR using Eqs. 4 and 5:

$$CHI:Lys = \frac{\frac{1}{5}A_{pyranose}}{\frac{1}{2}A_{lys\ A}} \quad (4)$$

$$CHI:Leu = \frac{A_{B+C} - 6\left(\frac{1}{2}A_{Lys\ A}\right)}{3} \quad (5)$$

where $A_{B+C} = 6*(1/2)A_{Lys\ A} + 3*A_{Leu\ C}$, $A_{pyranose}$ is the area of 5 protons on the pyranose ring of chitosan, $A_{Lys\ A}$ is the area of 2 alkyl protons on Lysine, and A_{B+C} is the area of 3 protons from leucine and 6 alkyl protons from lysine. The CHI:Lys ratio was determined to be 1:0.35 (Figure 6). With this information the ratio of CHI:Leu can be calculated using the resonance peak of B+C which consists of 6 lysine and 3 leucine protons. Upon substitution of $A_{Lys\ B}$ into Eq. 5 the CHI:Leu was found to be 1:0.22. Similarly, the extent of deprotection was found to be 39%.

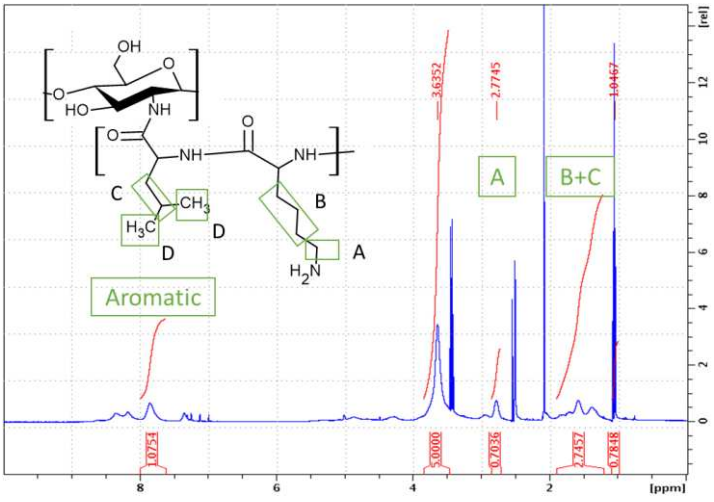

Figure 6. ^{1}H NMR spectra (d$_6$-DMSO) of CHI-graft-poly (lysine-co-leucine).

Synthesis of block GCPs

Amphiphilic GCPs with block sequences may adopt a number of conformations to as a result of various interactions with the local environment [29, 30]. Polypeptide block copolymers can be prepared in a one-pot synthesis where NCAs are sequentially added to the polymerization mixture. This technique allows for the synthesis of polymers with potentially complex structures that are often

Preprints (www.preprints.org) | NOT PEER-REVIEWED | Posted: 10 March 2023 doi:10.20944/preprints202303.0189.v1

poorly defined and difficult to characterize. In our work we synthesized the block graft copolymer, CHI-graft-Poly(Leucine-block-Lysine), in a two-step sequential graft copolymerization with NCA leucine and lysine, respectively (Figure 7). First, CHI initiated NCA-ROP of L-leucine at a ratio of 1:3 (CHI amino groups-to-NCA) to yield a CHI-g-poly(L-leucine) with a yield of >90%. The product was characterized with ^{1}H NMR to determine the actual ratio of CHI:Leu. However, the peaks associated with the CHI backbone protons were difficult to observe due to matrix effects. We observed such silencing of CHI. This is due to the fact that free CHI is insoluble in a solvent and the graft copolymer adopts a conformation where CHI collapses while the sidechains swell thus providing solubility of the entire macromolecule. On second step, CHI-g-poly(L-leucine) was subjected to NCA-ROP of L-lysine(Z). Ideally, only the amino groups present on the propagating ends of the polyleucine will initiate polymerization. However, unreacted amino groups on CHI may also serve as grafting sites yielding blocks of poly(L-lysine) directly attached to the CHI backbone. Regardless, the resulting product will still adopt configurations that maximize favorable interactions with the environment and access novel conformations and assemblies. Upon work up, the ratio of the amino acid blocks to CHI was evaluated with ^{1}H NMR using Equations 5 and 6:

$$Chi{:}\,Lysine = \left[\left(\frac{\frac{1}{5} * A_{Pyranose}}{\frac{1}{2} * \left(A_{Lys\,A}\right)}\right)\right] \quad (6)$$

=where, $A_{pyranose}$ is the area of 5 protons on the pyranose ring of chitosan, $A_{Lys\,A}$ is the area of 2 alkyl protons on Lysine, and A_{B+C} is the area of 3 protons from leucine and 6 alkyl protons from lysine. The CHI:Lysine ratio was determined to be 1:0.65 from Equation (6). With this information, the ratio of CHI:Leu was calculated using the combintion of peaks of B+C which consists of 6 lysine and 3 leucine protons. Upon substitution of $A_{Lys\,A}$ into Equation (5) the CHI:Leu was found to be 1:0.31. Similarly, the extent of Cbz-deprotection was determined to be 45% by evaluating the resonances $A_{aromatic}$ and $A_{Lys\,A}$ (Figure 8). It is important to note that this value may be underestimated due to matrix effects. The graft copolymer can adopt conformations that place protected and deprotected lysine in distinct environments.

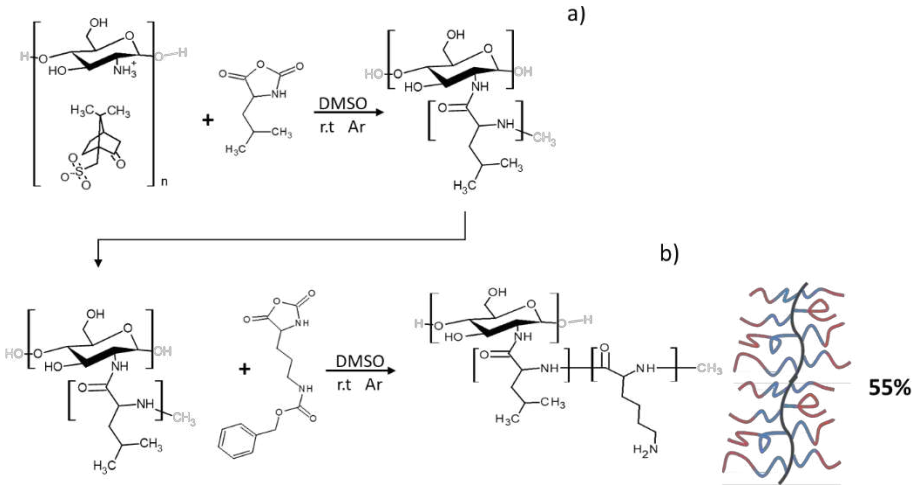

Figure 7. Synthesis of Chitosan-graft-Poly(L-leucine-block-L-lysine) ("Block") via sequential ring-opening polymerization of L-leucine (a) and L-lysine(Z) (b) in a two-step process.

Preprints (www.preprints.org) | NOT PEER-REVIEWED | Posted: 10 March 2023 doi:10.20944/preprints202303.0189.v1

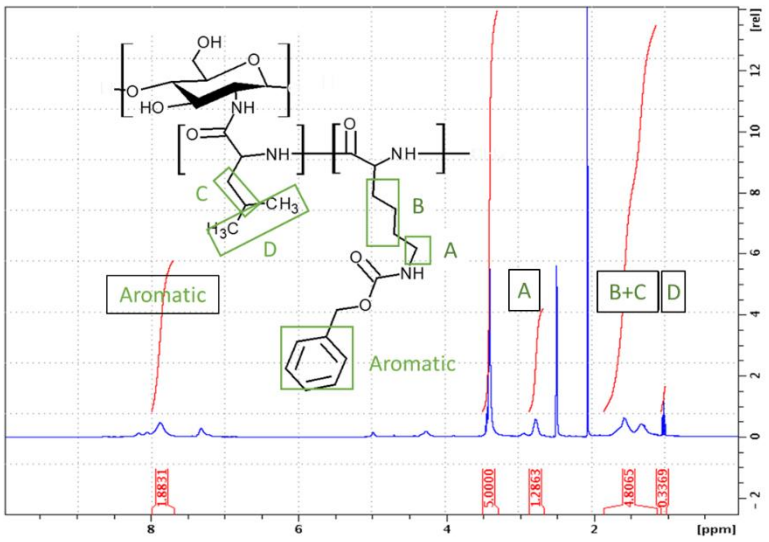

Figure 8. ^{1}H NMR spectra (d$_6$-DMSO) of CHI-graft-poly (L-lysine-block-L-leucine).

In conjunction with CHI-graft-Poly(L-leucine-block-L-lysine), which has a hydrophobic core and cationic shell, we made an attempt to synthesize CHI-graft-Poly (L-lysine-block-L-leucine) "reverse-block". The polymer has been successfully obtained and isolated. Unfortunately, upon deprotection it was not soluble in water and thus could not be used any further.

FTIR spectroscopic analysis was employed to characterize the final products and confirm the grafting of the peptide chains (Figure 9). CHI was evaluated and compared after each step of the synthesis. In all spectra the absorbance of amide bands I (1676 cm^{-1}), II (1531 cm^{-1}), and III (1252 cm^{-1}) appear after ROP, supporting the successful grafting of polypeptides. Additionally, the disappearance of the C-O-C benzyl stretch upon deprotection indicates the removal of the carboxybenzyl group from grafted polylysine.

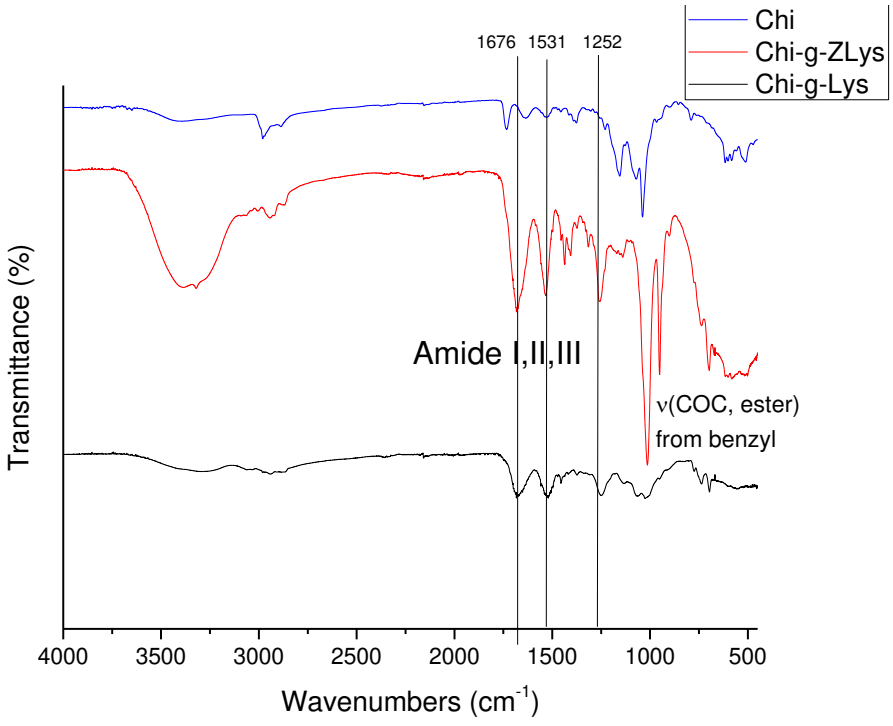

Figure 9. Representative FTIR spectra of CHI-CSA (blue), CHI-graft-Poly(L-lysine(Z)) (red), and CHI-graft-Poly (L-lysine) (black).

Preprints (www.preprints.org) | NOT PEER-REVIEWED | Posted: 10 March 2023 doi:10.20944/preprints202303.0189.v1

We used SEC to assess the molecular weight of some of the products. In general, characterization charged polymers with SEC poses substantial challenges caused by specific interactions of the polymer and the stationary phase of the column, and a lack of standards that accurately represent the hydrodynamic radius of nonlinear molecules and polyelectrolytes [31, 32]. We used aprotic solvent DMF in order to minimize ionization of the polymeric products. Only two products were soluble in DMF: CHI-graft-Poly(L-lysine) and a linear model compund GlcN-term-poly(lysine)). Our attempts to use SEC for this and other compunds dissolved in water resulted in extremely low elution volumes corrsponding to high molecular weights beyond any possibility which indicated either strong ionization of the products or formation of aggregates.

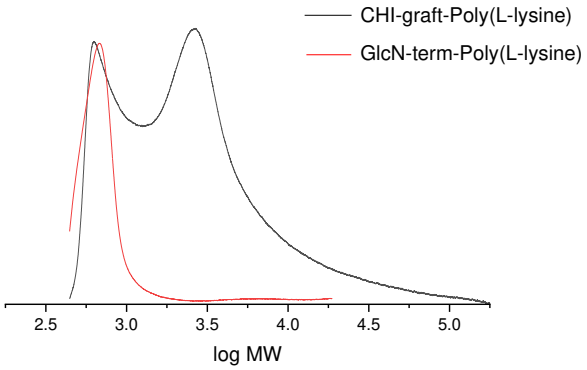

Figure 10. SEC of CHI-graft-Poly(L-lysine) (black) and a linear model compund GlcN-term-poly(lysine)) (red) in DMF.

The results of SEC of CHI-graft-Poly(L-lysine) and GlcN-term-poly(L-lysine)) are shown in Figure 10. The molecular weight of GlcN-term-poly(L-lysine)) is 627 g/mol. Taking into account the weight of terminal GlcN fragment 178 g/mol, we determine the length of poly(L-lysine) is about 3.5 units. This finding fits well with the synthesis when 3-fold (molar) amount of lysine(Z) NCA monomer was added to GlcN initiator. Some amount of GlcN-term-poly(L-lysine)) is also observed on the SEC of CHI-graft-Poly(L-lysine), while the main broad peak has averaged 3250 g.mol. Taking into account the molar ratio 1:0.65 of CHI and L-lysine from NMR, we obtain ave. 2.5 poly(L-lysine) chains of ave. 3.5 units long grafted to CHI backbone composed of 13 units of glucosamine.

Antimicrobial Activity

Following the characterization of all of our products, we examined the antimicrobial activity of our graft-copolymers. AMPs preferentially bind to the plasma membrane bilayer (PMB) of bacteria through electrostatic interactions. The selectivity in binding arises from differences in the relative abundance and distribution of charged and hydrophobic phospholipids. In line with this model, many reports cite that an optimum level of hydrophobicity is required to sufficiently facilitate interactions with fatty acyl chains to trigger membrane permeabilization [33]. However, AMPs with increased hydrophobic content can bind to mammalian membranes and exhibit increased toxicity [34].

In the case of chitosan-graft-polypeptides, several variables create a more complex picture of selectivity. For example, many of the naturally occurring antimicrobial peptides characterized to date possess a net positive charge, ranging from +2 to +9 [35], whereas the GCPs in this work potentially carry more positive charges per macromolecule. From this perspective, they may bind to cells irrespective of their composition and greatly reduce selectivity or efficiency. Additionally, if the GCPs do in fact deliver a high local concentration of peptide mass to the membrane interface, then off-target interactions with host cells could trigger cell death and lead to increased cytotoxicity. However, membrane adsorption is a poorly defined process in a complex environment. Off-target interactions such as protein adsorption and cation screening may substantially affect the electrostatic potential of the GCP. Additionally, outside the cytoplasmic membrane of both Gram-negative and Gram-positive

 doi:10.20944/preprints202303.0189.v1

bacteria, there is a peptidoglycan layer consisting of glycan chains interconnected by peptide side chains [36]. GCPs in this work mimic the composition of bacteria cell walls and may provide complementary interactions in that environment. This additional structural affinity may promote selectivity and offset hydrophobic binding to mammalian cells.

Finally, due to the large molecular weight of the GCPs small changes in the mole fraction of its components can lead to dramatic changes in adsorption behavior. All these traits combined make it difficult to target compositions that exhibit strong selectivity. With this in mind, the synthesized chitosan-graft-polypeptides were initially screened for cytotoxicity.

The colorimetric MTT assay was utilized to assess mammalian cell biocompatibility and in vitro cytotoxicity. In this experiment the GCPs were tested against Human Dermal Fibroblasts (HDF) cells. HDF cell were chosen as they are widely used as model to mimic the interaction of materials with human skin. They are also key components in inflammatory processes and wound healing. Due to the large molecular weight of GCPs they are likely best suited for topical applications rather than systemic administration. The cytotoxicity GCPs against HDF cells was evaluated over more common hemolytic activity.

In general, CHI-graft-Poly(L-lysine), exhibited the lowest toxicity with a minimum cell viability of 65% at 30 mg/ml. Glucosamine terminiated poly(lysine) was slightly more toxic with 50% viability at 30 mg/ml. CHI-graft-poly(Lys-co-Leu) and CHI-graft-poly(Leu-block-Lys) exhibited similar profiles and were substantially more toxic with nearly 90% cell death at the solubility limit of 30 mg/ml (See Supplementary Information, Figure S1). In the case of all four compounds, however, 2.5 mg/ml was found to have no-to-little effect on HDF viability. Equipped with this information antibacterial assays of the GCPs were conducted at concentrations below 2.5 mg/ml for therapeutic relevance.The antimicrobial activity of GCP's against Escherichia coli and Staphylococcus aureus was determined using microtiter dilution methods. For each graft copolymer and GLU-term-p(Lys), the minimal inhibitory concentration (MIC) was determined as the lowest concentration of polymer to inhibit 90% of bacteria after overnight incubation. Reductions in the growth of E. coli and S. aureus vs polymer concentration are shown in Figures 11 and 12, respectively, and represent the average of at least 12 trials. MIC values were quantified using a nonlinear regression method adapted from Lambert et al. [37] and reported in Table 2.

The minimum bactericidal concentration (MBC) was determined using alamarBlue cell viability reagent. When added to bacteria, alamarBlue is modified by the reducing environment of viable cells and turns red. Wells with the lowest polymer concentration which do not change color correspond to the MBC. The MBC was also confirmed by subculturing wells with the lowest concentration of polymer that inhibited growth onto agar plates. Plates that did not show bacteria growth after overnight incubation corresponds to the MBC (Figure 12). Further details of the antimicrobial assay procedure are given in the material and methods section.

Our results show that all the polymers can inhibit in vitro growth of E. coli but are largely inactive against S. aureus (Table 2). At the highest concentrations, CHI-graft-poly(L-lysine) was observed to reduce E. coli growth by 50% (Figure 11). Despite possessing hydrophobic content from the chitosan backbone, CHI-graft-poly(L-lysine) probably lacked sufficient hydrophobicity to efficiently compromise membrane integrity. CHI-graft-poly(Leu-block-Lys) and CHI-graft-poly(Lys-co-Leu), on the other hand, showed a nearly complete reduction in bacteria growth at similar concentrations. CHI-g-poly(Lys-co-Leu) was found to be twice as potent as CHI-g-poly(Leu-block-Lys) despite having similar amino acid composition. Though the overall activity was similar, differences are consistent with the hypothesis that block copolymer architectures may facilitate membrane permeabilization compared to homogeneous copolymers. However, further study with greater contrast between block and copolymer composition is needed. Despite these promising results, the GCPs are inactive against S. aureus (Figure 12). This is likely due to the presence of a thick peptidoglycan layer on the outer membrane of gram-positive bacteria which can prevent the diffusion of large molecules.

Preprints (www.preprints.org) | NOT PEER-REVIEWED | Posted: 10 March 2023 doi:10.20944/preprints202303.0189.v1

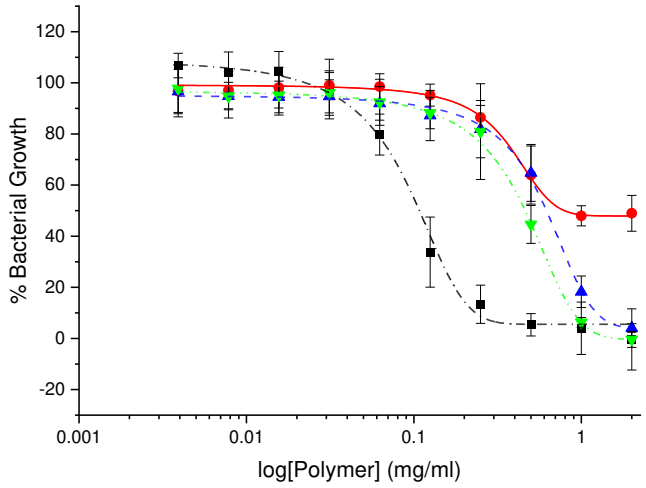

Figure 11. Growth inhibition curve of E. coli treated with different concentrations of glucosamine-terminated poly(lysine) (black squares), CHI-graft-poly(lysine) (red circles), Chi-graft-poly(lysine-co-leucine) (blue triangles), and Chi-graft-poly (leucine-block-lysine) (green triangles) for 24hrs. Data are presented as the mean ± standard deviation, n=12.

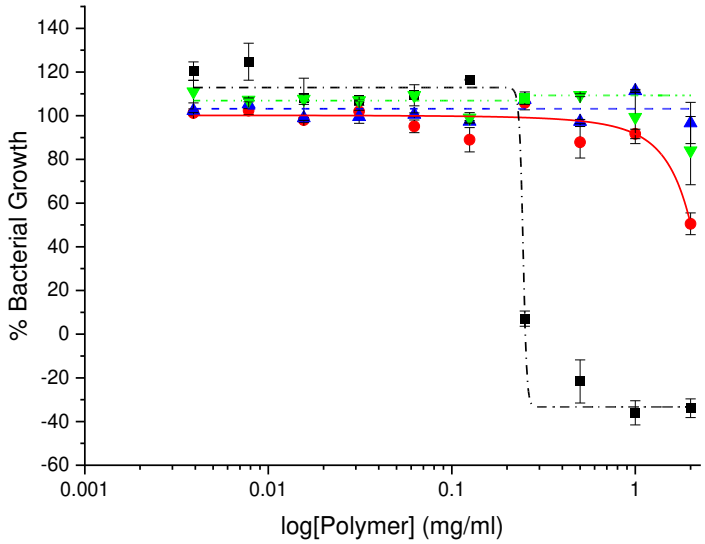

Figure 12. Growth inhibition curve of S. aureus treated with different concentrations of GlcN-term-poly(lysine) (black squares), CHI-graft-poly(lysine) (red circles), CHI-graft-poly(lysine-co-leucine) (blue triangles), and CHI-graft-poly(leucine-block-lysine) (green triangles)) for 24hrs. Data are presented as the mean ± standard deviation, n=12.

GlcN-term-poly(L-lysine) effectively inhibited in vitro growth of E. coli and S. aureus at concentrations well below the graft copolymers MIC (Table 2). Similar end-tethered oligo-Lysine structures synthesized by Singla et al. [38], exhibit comparable antimicrobial activity and were found to induce membrane damage in the tested microbes. Given GlcN-term-poly(L-lysine) biocompatibility and activity further optimization of such scaffolds could prove to be effective antimicrobial agents. It is important to note that differences in activity between GlcN-term-poly(L-lysine) and the graft copolymers may be exaggerated from expressing the MIC in terms of mg/ml

Preprints (www.preprints.org) | NOT PEER-REVIEWED | Posted: 10 March 2023 doi:10.20944/preprints202303.0189.v1

rather than μM. Graft copolymers have a substantially larger molecular weight which equates to fewer molecules per gram compared to GlcN-term-poly(L-lysine).

Table 2. Minimum Inhibitory Concentrations (MICs) **and** minimum bactericidal concentration (MBC) of polymers, mg/mL. The values are average of three replicates.

Polymer	*E. coli*		*S. aureus*	
	MIC	**MBC**	**MIC**	**MBC**
GlcN-term-poly(L-lysine)	0.16±0.09	0.25	N/A	0.25
CHI-graft-poly(L-lysine)	0.65±0.11	N/A	>2.0	>2.0
CHI-graft-poly(Lys-co-Leu)	1.2±0.02	2.0	>2.0	>2.0
CHI-graft-poly(Lys-block-Leu)	0.76±0.04	1.0	>2.0	>2.0
Magainin II	0.04±0.03	0.06	Not tested	

MBC was evaluated by subculturing the broth dilution of the MIC test. Wells above and below the respective MIC were subcultured onto agar plates and incubated for 24 hr. As seen in Figure 14, plates inoculated with GlcN-term-poly(L-lysine), CHI-graft-poly(Lys-co-Leu), and CHI-graft-poly(Lys-block-Leu) at the respective MIC concentration did not proliferate. However, CHI-graft-poly(L-lysine) showed growth at 2.0 mg/ml which agrees with MIC data.

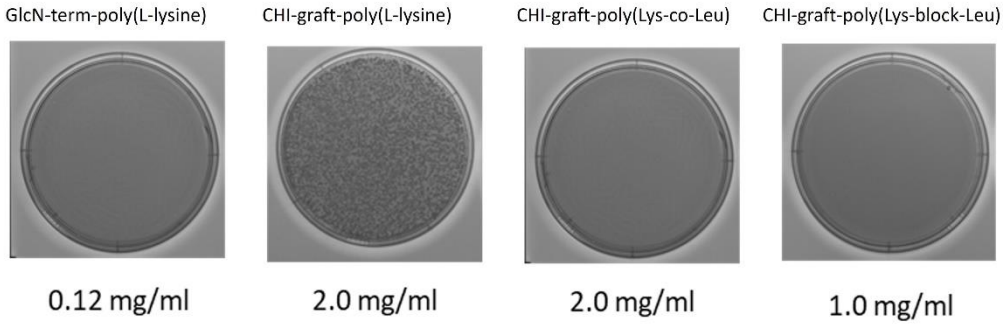

Figure 13. MBC Plates. E. coli cultures with the lowest concentration of graft copolymer that exhibited no change in growth were subcultured to determine minimum bactericidal concentrations. Each image displays bacteria growth on Mueller-Hinton agar plates after 24 hrs incubation. Note 2.0 mg/ml was the highest concentration tested and is below the MIC of CHI-graft-poly(L-lys).

Another factor potentially influencing the antimicrobial activity of GCPs is the formation of aggregates such as micelles. Amphiphilic polymers form micelles in aqueous solution whereby the polar region faces the outside surface, and the nonpolar region forms the core. In this state the antimicrobial activity of GCPs may be substantially affected. Additionally, the formation of micelles corresponds to changes in optical properties such as light scattering which may impact absorbance measurements in the MIC assay. In order to determine if the GCPs form micelles at concentration relevant to the MIC the optical absorbance was evaluated over increasing concentrations of polymer in MH media (Figure 13). Both GlcN-term-poly(L-lysine) and CHI-graft-poly(L-lysine) demonstrated non-linear scattering which indicate the formation of micelles. CHI-g-p(Lys-co-Leu) and CHI-g-p(Leu-block-Lys) on the other hand did not exhibit a change in slope over relevant concentrations. This may explain why GlcN-term-poly(L-lysine) effectively inhibited in vitro growth of E. coli and S. aureus at concentrations well below the graft copolymers MIC.

Preprints (www.preprints.org) | NOT PEER-REVIEWED | Posted: 10 March 2023 doi:10.20944/preprints202303.0189.v1

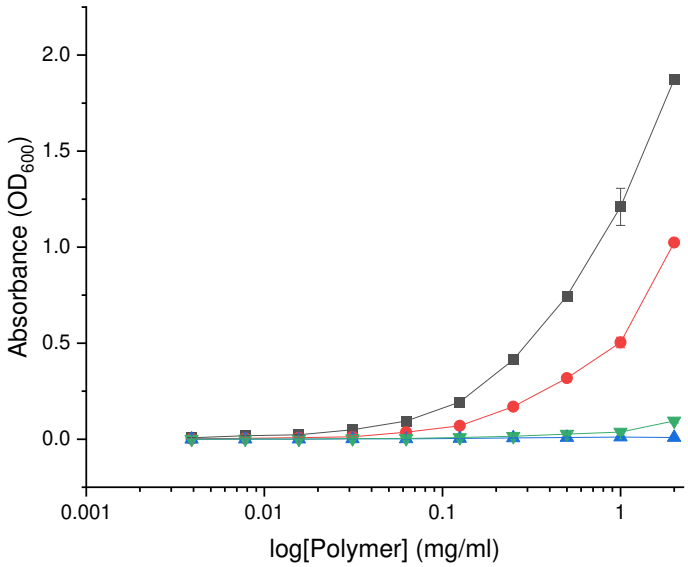

Figure 14. Absorbance of the graft copolymers at varying concentration in MH media at 600nm: GlcN-term-poly(lysine) (black squares), CHI-graft-poly(lysine) (red circles), CHI-graft-poly(lysine-co-leucine) (blue triangles), and CHI-graft-poly(leucine-block-lysine) (green triangles) for 24hrs. Data are presented as the mean ± standard deviation, n=4.

Biofilms consist of an assembly of microorganisms embedded in a self-produced matrix of extracellular polymeric substances (EPSs) containing polysaccharides, extracellular DNA, proteins, and lipids [39]. The EPS layer acts as a sort of a "glue" adhering the cells to one another and shields bacteria from harsh environmental conditions. In this protected scaffold biofilm-associated cells grow significantly slower and enter a non-replicating dormant state. As a result, biofilm-embedded bacteria exhibit strong antibiotic resistance and typically require 1000-fold higher concentrations to be effective [40].

Biofilms are of clinical relevance due to their ability to colonize medical devices such as catheters and implants. The National Institutes of Health in the USA reported that approximately 80% of chronic infections in humans are biofilm-related [41]. Due to the unique characteristics of biofilm and its role in human diseases, an urgent need exists for effective treatments.

AMP-mediated strategies for biofilm eradication are an attractive approach that has gained attention in recent years. Compared to traditional small-molecule antibiotics AMPs offer fast-killing kinetics, a high potential to act on slow-growing or non-growing bacteria, and the ability to synergize with antibiotics [42]. Antimicrobial peptides and polymers have been reported to act at several stages of biofilm development and with different mechanisms of action.

Depending on the stage of development the AMP targets it may inhibit the formation or eradicate established biofilms. AMPs that follow an inhibitory pathway typically do so by; (1) altering the adhesion of microbial cells by binding their surface or the surface of the substrate, [43] (2) disrupting signaling molecules that regulate biofilm formation [44], or (3) killing early colonizer cells to prevent biofilm maturation [45].

AMPs that target established biofilms follow mechanisms that either kill microbial cells or reduce biofilm mass. Killing pathways typically do so by penetrating the EPS matrix and inhibiting cell division or, disrupting the cytoplasmic membrane of microbial cells directly [46]. AMPs that eradicate biofilms reduce film mass by solubilizing components of the EPS matrix via its amphipathic and cationic structure [47].

We studied the potential of cationic peptidopolysaccharide graft copolymers to act as an anti-biofilm agent. In addition to antimicrobial activity, the synthesized GCPs readily form micelles that may support the solvation of key components in the ECM matrix. Similar materials have been found to act as compatibilizers, stabilizing the solvation of immiscible blends [48, 49]. Additionally, the

Preprints (www.preprints.org) | NOT PEER-REVIEWED | Posted: 10 March 2023 doi:10.20944/preprints202303.0189.v1

cationic and hydrophobic motifs may promote favorable interaction with the outer membrane of bacteria and neutralize surface charges. Finally, the GCPs may adsorb onto biofouling surfaces before colonization or directly on the biofilm and prevent further development.

Herein, we evaluated the anti-biofilm activity of the graft copolymers series against Agrobacterium tumefaciens (A. tumefaciens). A. tumefaciens was selected as a model bacterium as it readily forms biofilms, is generally safe to humans and has well-established assays and protocols for evaluation.

The anti-biofilm activity of the GCPs was evaluated by inoculating wild type A. tumefaciens and the mutants ΔvisR and Δupp before colonizing the substrate surface. The deletion mutants ΔvisR and Δupp were included as controls and exhibit increased and decreased biofilm production respectively. Changes in biofilm mass were quantified using a static biofilm coverslip assay optimized for A. tumefaciens [18, 50]. Briefly, the agrobacterium strains were cultured overnight and diluted to an optical density of 0.05 A.U. in 35mm wells. The cultures were inoculated to a concentration of 0.25 mg/ml with the respective GCP and a polyvinyl chloride coverslip was suspended in the solution. After 24hrs incubation planktonic bacteria growth was quantified by spectrophotometry and the colonized coverslips were stained with crystal violet solution. Images of the stained biofilms were collected for qualitative analysis. Finally, crystal violet was solubilized from the films and the absorbance was measured at 600nm to estimate the relative amounts of adhered biomass.

Adherent biofilm mass after treatment with the respective graft copolymers is shown in Figure 15. When compared to untreated, both GlcN-term-poly(L-lysine) and CHI-graft-poly(Lys-co-Leu) showed significant reductions in the adherent mass of WT and ΔvisR strains. CHI-graft-poly(Leu-block-Lys) on the other hand, increased biofilm mass of wild type while decreasing ΔvisR. No changes were observed in the biofilms of the Δupp strain for any of the graft copolymers. Given that Δupp lacks the exopolysaccharide adhesions that are critical for surface attachment, exposure to the graft copolymers could only result in increased adherent mass.

Differences in the activity of CHI-graft-poly(Leu-block-Lys) when exposed to wild type or ΔvisR are unexpected. However, antimicrobial peptides are known to target a wide range of intracellular components, including, DNA, RNA, and proteins [51]. Binding to any of these sites is complex as it can lead to opposing trends in biofilm regulation. Subtle changes in gene expression or the intracellular composition of ΔvisR may facilitate graft copolymer binding and alter biofilm expression.

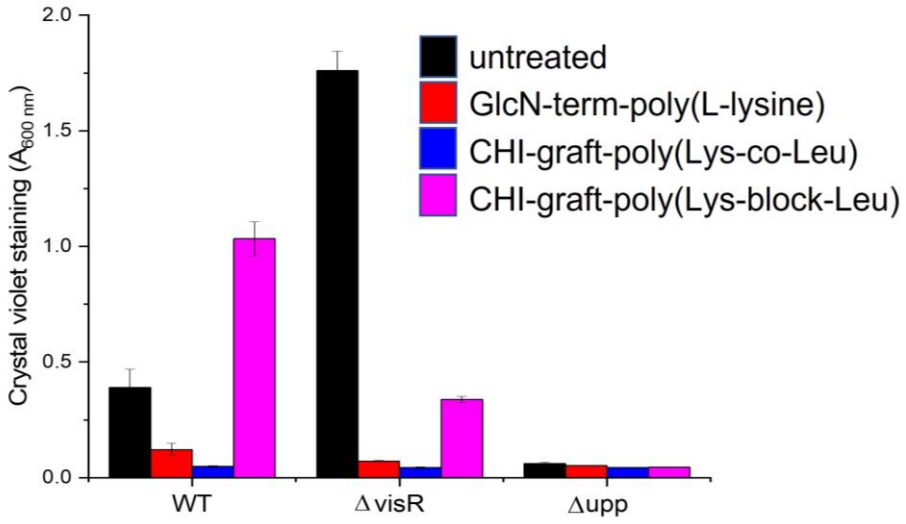

Figure 15. Inhibition of adherent biomass upon exposure to cationic peptidopolysaccharide graft copolymers. A. tumefaciens was grown in the presence of the respective graft copolymers at a concentration of 0.25 mg/ml. The ΔvisR and Δupp mutants exhibit enhanced and depleted film formation respectively. Total adherent biomass was quantified by crystal violet staining. Mean values of three independent experiments and standard error are shown.

Preprints (www.preprints.org) | NOT PEER-REVIEWED | Posted: 10 March 2023 doi:10.20944/preprints202303.0189.v1

The direct antimicrobial effects of the graft copolymers on planktonic A. tumefaciens were also evaluated. Optical density measurements of the biofilm inoculum were taken before and after film formation (Figure 16). Reductions of 50% or greater were observed for all graft polymers and strains of bacteria. This implies that direct antimicrobial activity of the GCPs in solution may contribute to biofilm losses.

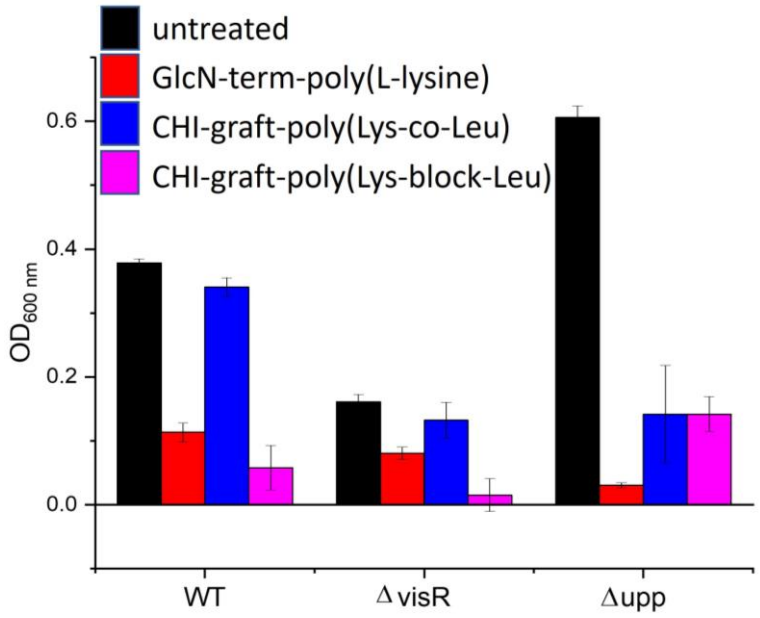

Figure 16. Optical density of A. tumefaciens planktonic biomass treated with 0.25 mg/ml of each polymer. Values are averages of triplicate assays and error bars represent standard deviation.

The extent to which reductions in biofilm mass correspond to reductions in planktonic bacteria was evaluated by normalizing the ratio of biofilm mass to the number of planktonic bacteria (Figure 17). Values greater than 100% correspond to elevated biofilm formation, while values less than 100% indicate the biofilm is disproportionately reduced relative to viable planktonic bacteria.

Wild type A. tumefaciens treated with glucosamine-terminated poly(lysine) exhibited reductions in biofilm mass and planktonic bacteria that are in proportion to untreated. This suggests the anti-biofilm activity of GLU-term-p(Lys) is a result of antimicrobial action rather than selective inhibition. CHI-g-p(Lys-co-Leu) on the other hand, reduced adherent mass without killing planktonic bacteria. Finally, CHI-g-p(Leu-block-Lys) was found to increase adherent mass despite reducing viable bacteria. Further investigation is required to understand the mechanism of this paradoxical behavior.

Preprints (www.preprints.org) | NOT PEER-REVIEWED | Posted: 10 March 2023 doi:10.20944/preprints202303.0189.v1

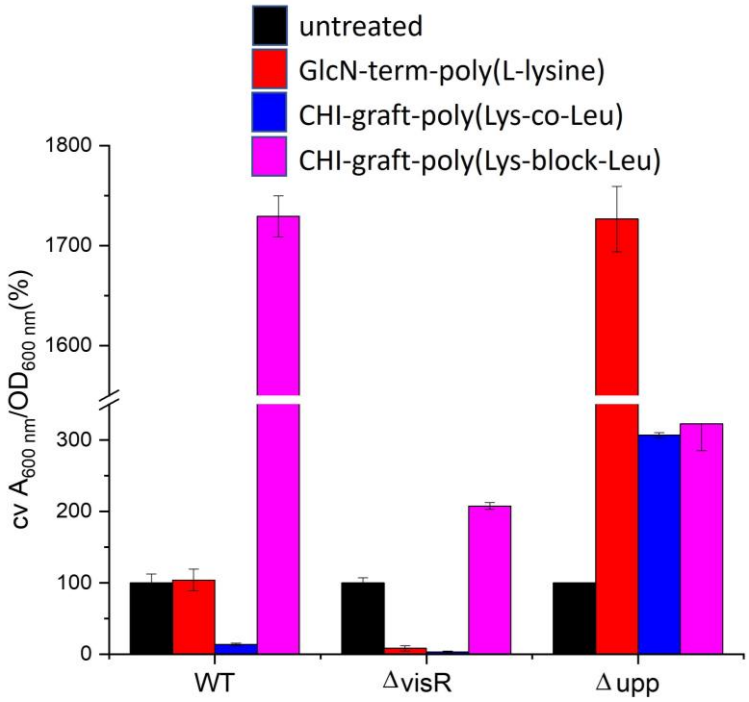

Figure 17. Changes in adherent biofilm mass (A_{600}) of A. tumefaciens normalized by planktonic biomass (OD_{600}) treated with 0.25 mg/ml of each polymer. Values are averages of triplicate assays and error bars represent standard deviation. Data for each strain are normalized (100%) to non-treated cultures of each strain (black bars).

4. Conclusions

In conclusion, this work describes the synthesis and characterization of cationic peptidopolysaccharide graft copolymers. Utilizing a "grafting from" approach the hydrophobic and cationic amino acids were conjugated to the polysaccharide chitosan via ring opening polymerization of NCA-amino acids. The polymers were designed as a novel antimicrobial agent that adheres to traditional structure-function relationships of AMPs while also mimicking the peptidoglycan structure of bacteria. GCPs with block copolymer peptide chains were successfully synthesized in a two-step sequential synthesis. Several amino acid combinations and sequences were synthesized however CHI-*graft*-poly(lysine), CHI-*graft*-poly(lysine-*co*-leucine), and CHI-*graft*-poly (leucine-*block*-lysine) were optimal for further study. The extent of modification of chitosan was determined using mass spectrometry and NMR spectroscopy. The structure of the graft copolymers likely consists of a peptide chain (3 to 12 amino acids long) for every 10 CHI repeating units.

Additionally, the antimicrobial activity and biocompatibility of cationic peptidopolysaccharide graft copolymers were evaluated. Compared to linear antimicrobial polymers GCPs have greater conformational freedom and charge density which may lead to enhanced bactericidal activity and unique modes of action. Additionally, GCPs with a peptidopolysaccharide composition may have favorable interactions with the peptidoglycan layer present in bacteria cell walls. A small set of representative polymers, CHI-*graft*-poly(lysine), CHI-*graft*-poly(lysine-*co*-leucine), and CHI-*graft*-poly(leucine-*block*-lysine), along with glucosamine-terminated poly(lysine) were selected for study. The in vitro cytotoxicity of the GCPs was evaluated against human dermal fibroblasts (HDF). Of the screen compounds, glucosamine-terminated poly(lysine) and CHI-*g*-p(Lys) exhibited the lowest toxicity. All four polymers demonstrated good cytocompatibility at 2.5 mg/ml. All the polymers were found to inhibit *in vitro* growth of *E. coli* but are largely inactive against *S. aureus.* CHI-*g*-p(Lys-co-Leu) was found to be twice as potent as CHI-*g*-p(Leu-*block*-Lys). GLU-*term*-p(Lys) effectively inhibited *in vitro* growth of *E. coli* and *S. aureus* at concentrations well below the graft copolymers MIC. The anti-biofilm activity of the GCPs was evaluated against *Agrobacterium tumefaciens* (*A.*

tumefaciens), a plant pathogen of agricultural relevance. Both GLU-term-p(Lys) and CHI-*g*-p(Lys-co-Leu) showed significant reductions in the adherent mass of WT and Δ*visR* strains. CHI-*g*-p(Leu-block-Lys) on the other hand, increased biofilm mass of wild type while decreasing Δ*visR*. The extent to which reductions in biofilm mass correspond to reductions in planktonic bacteria was evaluated by normalizing the ratio of biofilm mass to the number of planktonic bacteria. GLU-*term*-p(Lys) reduced adherent mass proportionally to cell viability whereas CHI-*g*-p(Lys-co-Leu) more selectively inhibited biofilm formation. Finally, CHI-*g*-p(Leu-*block*-Lys) was found to reduce planktonic cell viability while increasing adherent biofilm mass.

Supplementary Materials: The following supporting information can be downloaded at the website of this paper posted on Preprints.org. Figure S1: MTT cell viability assay results. Human Dermal Fibroblast (HDF) cells were exposed to the indicated concentrations of glucosamine-terminated poly(lysine) (black), CHI-graft-poly(lysine) (red), Chi-graft-poly(lysine-co-leucine) (blue), and Chi-graft-poly (leucine-block-lysine) (magenta) for 24hrs. Data are presented as the mean ± standard deviation, n=3.

Conflict of interests: The authors declare no conflict of interest.

Author Contributions: Conceptualization: A.S. and T.E.; methodology development: T.E. and J. H.; synthetic work and polymer characterization: T.E., G.S., and D.G.; antimicrobial characterization: T.E., D.G., and J.H.; writing—original draft preparation, T.E. and G.S. writing—review and editing, T.E., G.S., J.H., and A.S. All authors have read and agreed to the published version of the manuscript.

Data Availability Statement: All data generated or analysed during this study are included in this published article.

References

1. Diamond, G.; Beckloff, N.; Weinberg, A.; Kisich, K. O., The roles of antimicrobial peptides in innate host defense. *Curr Pharm Des* **2009,** *15* (21), 2377-92.
2. Fjell, C. D.; Hiss, J. A.; Hancock, R. E. W.; Schneider, G., Designing antimicrobial peptides: form follows function. *Nature Reviews Drug Discovery* **2011,** *11*, 37.
3. Brogden, K. A., Antimicrobial peptides: pore formers or metabolic inhibitors in bacteria? *Nature Reviews Microbiology* **2005,** *3* (3), 238-250.
4. Zhang, Q.-Y.; Yan, Z.-B.; Meng, Y.-M.; Hong, X.-Y.; Shao, G.; Ma, J.-J.; Cheng, X.-R.; Liu, J.; Kang, J.; Fu, C.-Y., Antimicrobial peptides: mechanism of action, activity and clinical potential. *Military Medical Research* **2021,** *8* (1), 48.
5. Han, Y.; Zhang, M.; Lai, R.; Zhang, Z., Chemical modifications to increase the therapeutic potential of antimicrobial peptides. *Peptides* **2021,** *146*, 170666.
6. D'Souza, A. R.; Necelis, M. R.; Kulesha, A.; Caputo, G. A.; Makhlynets, O. V., Beneficial Impacts of Incorporating the Non-Natural Amino Acid Azulenyl-Alanine into the Trp-Rich Antimicrobial Peptide buCATHL4B. *Biomolecules* **2021,** *11* (3).
7. Huang, K.-S.; Yang, C.-H.; Huang, S.-L.; Chen, C.-Y.; Lu, Y.-Y.; Lin, Y.-S., Recent Advances in Antimicrobial Polymers: A Mini-Review. *International journal of molecular sciences* **2016,** *17* (9), 1578.
8. Chang, H.-I.; Yang, M.-S.; Liang, M., The synthesis, characterization and antibacterial activity of quaternized poly(2,6-dimethyl-1,4-phenylene oxide)s modified with ammonium and phosphonium salts. *Reactive and Functional Polymers* **2010,** *70* (12), 944-950.
9. Palermo, E. F.; Kuroda, K., Chemical Structure of Cationic Groups in Amphiphilic Polymethacrylates Modulates the Antimicrobial and Hemolytic Activities. *Biomacromolecules* **2009,** *10* (6), 1416-1428.
10. Popa, A.; Davidescu, C. M.; Trif, R.; Ilia, G.; Iliescu, S.; Dehelean, G., Study of quaternary 'onium' salts grafted on polymers: antibacterial activity of quaternary phosphonium salts grafted on 'gel-type' styrene–divinylbenzene copolymers. *Reactive and Functional Polymers* **2003,** *55* (2), 151-158.
11. Costanza, F.; Padhee, S.; Wu, H.; Wang, Y.; Revenis, J.; Cao, C.; Li, Q.; Cai, J., Investigation of antimicrobial PEG-poly(amino acid)s. *RSC Advances* **2014,** *4* (4), 2089-2095.
12. Liu, L.; Xu, K.; Wang, H.; Jeremy Tan, P. K.; Fan, W.; Venkatraman, S. S.; Li, L.; Yang, Y.-Y., Self-assembled cationic peptide nanoparticles as an efficient antimicrobial agent. *Nat Nano* **2009,** *4* (7), 457-463.

13. Arnusch, C. J.; Branderhorst, H.; de Kruijff, B.; Liskamp, R. M. J.; Breukink, E.; Pieters, R. J., Enhanced Membrane Pore Formation by Multimeric/Oligomeric Antimicrobial Peptides. *Biochemistry* **2007,** *46* (46), 13437-13442.
14. Lam, S. J.; O'Brien-Simpson, N. M.; Pantarat, N.; Sulistio, A.; Wong, E. H. H.; Chen, Y.-Y.; Lenzo, J. C.; Holden, J. A.; Blencowe, A.; Reynolds, E. C.; Qiao, G. G., Combating multidrug-resistant Gram-negative bacteria with structurally nanoengineered antimicrobial peptide polymers. *Nature Microbiology* **2016,** *1*, 16162.
15. Hou, Z.; Shankar, Y. V.; Liu, Y.; Ding, F.; Subramanion, J. L.; Ravikumar, V.; Zamudio-Vázquez, R.; Keogh, D.; Lim, H.; Tay, M. Y. F.; Bhattacharjya, S.; Rice, S. A.; Shi, J.; Duan, H.; Liu, X.-W.; Mu, Y.; Tan, N. S.; Tam, K. C.; Pethe, K.; Chan-Park, M. B., Nanoparticles of Short Cationic Peptidopolysaccharide Self-Assembled by Hydrogen Bonding with Antibacterial Effect against Multidrug-Resistant Bacteria. *ACS Applied Materials & Interfaces* **2017,** *9* (44), 38288-38303.
16. Divyashree, M.; Mani, M. K.; Reddy, D.; Kumavath, R.; Ghosh, P.; Azevedo, V.; Barh, D., Clinical Applications of Antimicrobial Peptides (AMPs): Where do we Stand Now? *Protein Pept Lett* **2020,** *27* (2), 120-134.
17. Watson, B.; Currier, T. C.; Gordon, M. P.; Chilton, M. D.; Nester, E. W., Plasmid required for virulence of Agrobacterium tumefaciens. *J Bacteriol* **1975,** *123* (1), 255-64.
18. Xu, J.; Kim, J.; Koestler, B. J.; Choi, J. H.; Waters, C. M.; Fuqua, C., Genetic analysis of Agrobacterium tumefaciens unipolar polysaccharide production reveals complex integrated control of the motile-to-sessile switch. *Mol Microbiol* **2013,** *89* (5), 929-48.
19. Hitoshi, S.; Yoshihiro, S.; René, R., Dissolution of Chitosan in Dimethyl Sulfoxide by Salt Formation. *Chemistry Letters* **2000,** *29* (6), 596-597.
20. Smeets, N. M. B.; van der Weide, P. L. J.; Meuldijk, J.; Vekemans, J. A. J. M.; Hulshof, L. A., A Scalable Synthesis of l-Leucine-N-carboxyanhydride. *Organic Process Research & Development* **2005,** *9* (6), 757-763.
21. Weinhold, M. X.; Sauvageau, J. C. M.; Keddig, N.; Matzke, M.; Tartsch, B.; Grunwald, I.; Kübel, C.; Jastorff, B.; Thöming, J., Strategy to improve the characterization of chitosan for sustainable biomedical applications: SAR guided multi-dimensional analysis. *Green Chemistry* **2009,** *11* (4), 498-509.
22. Kasaai, M. R.; Arul, J.; Charlet, G., Fragmentation of Chitosan by Acids. *The Scientific World Journal* **2013,** *2013*, 508540.
23. Kurita, K.; Yoshida, A.; Koyama, Y., Studies on chitin. 13. New polysaccharide/polypeptide hybrid materials based on chitin and poly(.gamma.-methyl L-glutamate). *Macromolecules* **1988,** *21* (6), 1579-1583.
24. Chi, P.; Wang, J.; Liu, C., Synthesis and characterization of polycationic chitosan-graft-poly (l-lysine). *Materials Letters* **2008,** *62* (1), 147-150.
25. Yu, H.; Chen, X.; Lu, T.; Sun, J.; Tian, H.; Hu, J.; Wang, Y.; Zhang, P.; Jing, X., Poly(l-lysine)-Graft-Chitosan Copolymers: Synthesis, Characterization, and Gene Transfection Effect. *Biomacromolecules* **2007,** *8* (5), 1425-1435.
26. Perdih, P.; Pahovnik, D.; Cegnar, M.; Miklavžin, A.; Kerč, J.; Žagar, E., Synthesis of chitosan-graft-poly(sodium-l-glutamate) for preparation of protein nanoparticles. *Cellulose* **2014,** *21* (5), 3469-3485.
27. Dimitrov, I.; Schlaad, H., Synthesis of nearly monodisperse polystyrene–polypeptide block copolymers via polymerisation of N-carboxyanhydrides. *Chemical Communications* **2003,** (23), 2944-2945.
28. Knobler, Y.; Bittner, S.; Frankel, M., 749. Reaction of N-carboxy-α-amino-acid anhydrides with hydrochlorides of hydroxylamine, O-alkylhydroxylamines, and amines; syntheses of amino-hydroxamic acids, amido-oxy-peptides, and α-amino-acid amides. *Journal of the Chemical Society (Resumed)* **1964,** (0), 3941-3951.
29. Breedveld, V.; Nowak, A. P.; Sato, J.; Deming, T. J.; Pine, D. J., Rheology of Block Copolypeptide Solutions: Hydrogels with Tunable Properties. *Macromolecules* **2004,** *37* (10), 3943-3953.
30. Kwon, G. S.; Kataoka, K., Block copolymer micelles as long-circulating drug vehicles. *Advanced Drug Delivery Reviews* **1995,** *16* (2), 295-309.
31. Haidacher, D.; Horváth, C., Physicochemical Basis of Hydrophobic Interaction Chromatography. In *Theoretical Advancement in Chromatography and Related Separation Techniques*, Dondi, F.; Guiochon, G., Eds. Springer Netherlands: Dordrecht, 1992; pp 443-480.
32. Holbrook, R. D.; Galyean, A. A.; Gorham, J. M.; Herzing, A.; Pettibone, J., Chapter 2 - Overview of Nanomaterial Characterization and Metrology. In *Frontiers of Nanoscience*, Baalousha, M.; Lead, J. R., Eds. Elsevier: 2015; Vol. 8, pp 47-87.

33. Chen, Y.; Guarnieri, M. T.; Vasil, A. I.; Vasil, M. L.; Mant, C. T.; Hodges, R. S., Role of Peptide Hydrophobicity in the Mechanism of Action of α-Helical Antimicrobial Peptides. *Antimicrobial Agents and Chemotherapy* **2007,** *51* (4), 1398-1406.
34. Yin, L. M.; Edwards, M. A.; Li, J.; Yip, C. M.; Deber, C. M., Roles of hydrophobicity and charge distribution of cationic antimicrobial peptides in peptide-membrane interactions. *The Journal of biological chemistry* **2012,** *287* (10), 7738-45.
35. Yeaman, M. R.; Yount, N. Y., Mechanisms of Antimicrobial Peptide Action and Resistance. *Pharmacological Reviews* **2003,** *55* (1), 27.
36. Vollmer, W.; Blanot, D.; De Pedro, M. A., Peptidoglycan structure and architecture. *FEMS Microbiology Reviews* **2008,** *32* (2), 149-167.
37. Lambert, R. J.; Pearson, J., Susceptibility testing: accurate and reproducible minimum inhibitory concentration (MIC) and non-inhibitory concentration (NIC) values. *Journal of applied microbiology* **2000,** *88* (5), 784-90.
38. Singla, P.; Kaur, M.; Kumari, A.; Kumari, L.; Pawar, S. V.; Singh, R.; Salunke, D. B., Facially Amphiphilic Cholic Acid–Lysine Conjugates as Promising Antimicrobials. *ACS Omega* **2020,** *5* (8), 3952-3963.
39. Gomes Von Borowski, R.; Gnoatto, S. C. B.; Macedo, A. J.; Gillet, R., Promising Antibiofilm Activity of Peptidomimetics. *Frontiers in microbiology* **2018,** *9*, 2157.
40. Penesyan, A.; Nagy, S. S.; Kjelleberg, S.; Gillings, M. R.; Paulsen, I. T., Rapid microevolution of biofilm cells in response to antibiotics. *npj Biofilms and Microbiomes* **2019,** *5* (1), 34.
41. Jamal, M.; Ahmad, W.; Andleeb, S.; Jalil, F.; Imran, M.; Nawaz, M. A.; Hussain, T.; Ali, M.; Rafiq, M.; Kamil, M. A., Bacterial biofilm and associated infections. *Journal of the Chinese Medical Association : JCMA* **2018,** *81* (1), 7-11.
42. Herrmann, G.; Yang, L.; Wu, H.; Song, Z.; Wang, H.; Høiby, N.; Ulrich, M.; Molin, S.; Riethmüller, J.; Döring, G., Colistin-tobramycin combinations are superior to monotherapy concerning the killing of biofilm Pseudomonas aeruginosa. *The Journal of infectious diseases* **2010,** *202* (10), 1585-92.
43. Tan, Y.; Han, F.; Ma, S.; Yu, W., Carboxymethyl chitosan prevents formation of broad-spectrum biofilm. *Carbohydrate Polymers* **2011,** *84* (4), 1365-1370.
44. Overhage, J.; Campisano, A.; Bains, M.; Torfs, E. C.; Rehm, B. H.; Hancock, R. E., Human host defense peptide LL-37 prevents bacterial biofilm formation. *Infection and immunity* **2008,** *76* (9), 4176-82.
45. Arslan, S. Y.; Leung, K. P.; Wu, C. D., The effect of lactoferrin on oral bacterial attachment. *Oral microbiology and immunology* **2009,** *24* (5), 411-6.
46. Hou, S.; Zhou, C.; Liu, Z.; Young, A. W.; Shi, Z.; Ren, D.; Kallenbach, N. R., Antimicrobial dendrimer active against Escherichia coli biofilms. *Bioorganic & Medicinal Chemistry Letters* **2009,** *19* (18), 5478-5481.
47. Park, S.-C.; Lee, M.-Y.; Kim, J.-Y.; Kim, H.; Jung, M.; Shin, M.-K.; Lee, W.-K.; Cheong, G.-W.; Lee, J. R.; Jang, M.-K., Anti-Biofilm Effects of Synthetic Antimicrobial Peptides Against Drug-Resistant Pseudomonas aeruginosa and Staphylococcus aureus Planktonic Cells and Biofilm. *Molecules* **2019,** *24* (24), 4560.
48. Hall-Edgefield, D. L.; Shi, T.; Nguyen, K.; Sidorenko, A., Hybrid Molecular Brushes with Chitosan Backbone: Facile Synthesis and Surface Grafting. *ACS Applied Materials & Interfaces* **2014,** *6* (24), 22026-22033.
49. Vernaez, O.; Neubert, K. J.; Kopitzky, R.; Kabasci, S., Compatibility of Chitosan in Polymer Blends by Chemical Modification of Bio-based Polyesters. *Polymers (Basel)* **2019,** *11* (12), 1939.
50. Xu, J.; Kim, J.; Koestler, B. J.; Choi, J.-H.; Waters, C. M.; Fuqua, C., Genetic analysis of Agrobacterium tumefaciens unipolar polysaccharide production reveals complex integrated control of the motile-to-sessile switch. *Molecular Microbiology* **2013,** *89* (5), 929-948.
51. Cho, J. H.; Sung, B. H.; Kim, S. C., Buforins: Histone H2A-derived antimicrobial peptides from toad stomach. *Biochimica et Biophysica Acta (BBA) - Biomembranes* **2009,** *1788* (8), 1564-1569.